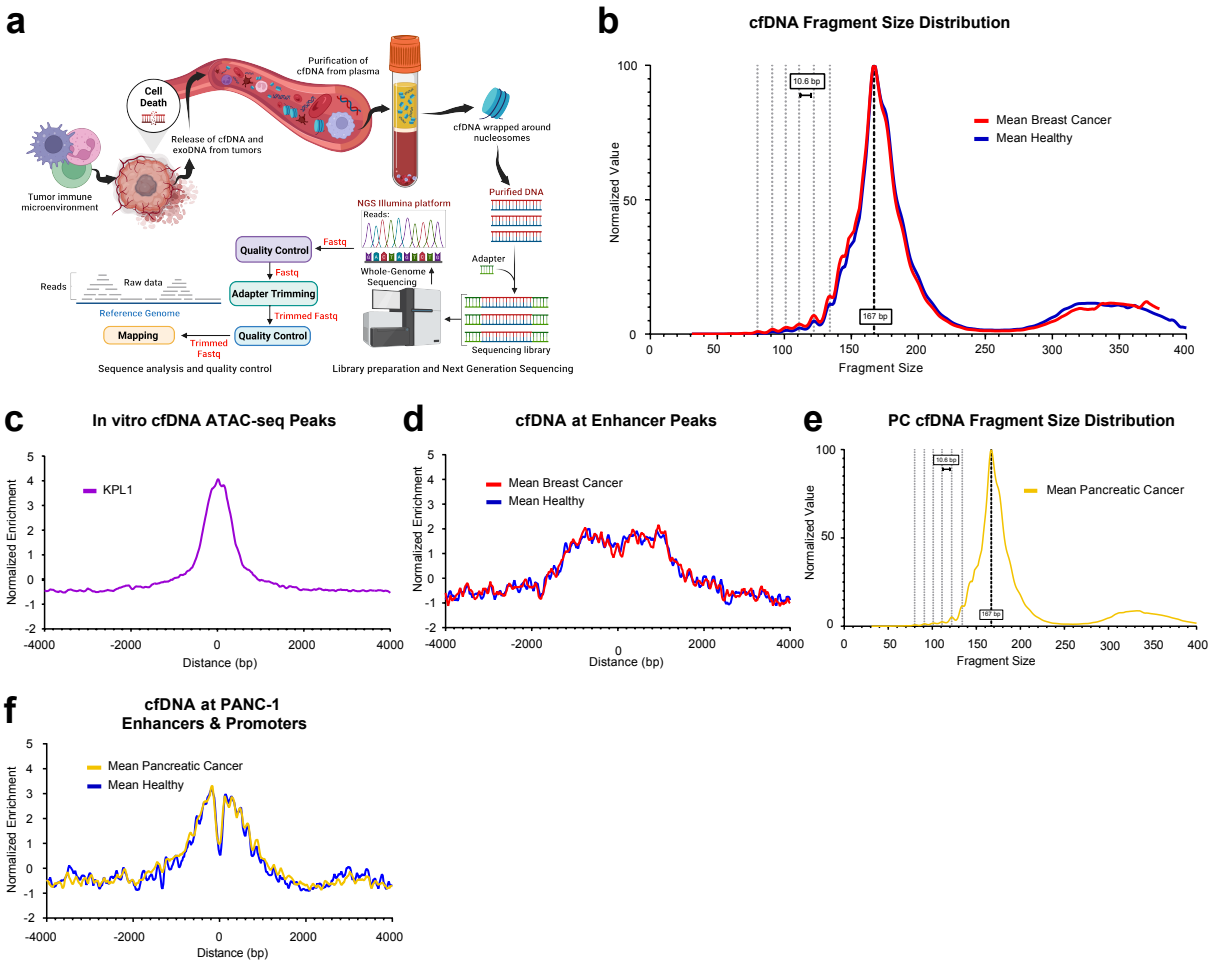

Supplementary Figure 1

a. Workflow Overview. cfDNAs were isolated from plasma, followed by library preparation and next-generation sequencing. **b.** Fragment size distribution of cfDNA. Mean fragment sizes from each group were normalized and scaled from 0 to 100 for comparison and plotted. **c.** Metaplot of *in vitro* cfDNAs at T47D ATAC-seq peaks. cfDNAs were purified from KPL1 cell culture medium and analyzed to show enrichment at open chromatin. **d.** Comparison of cfDNA enrichment at breast cancer enhancers between breast cancer patients and healthy individuals **e.** Fragment Size Distribution of cfDNAs isolated from pancreatic cancer patient plasma. **f.** Metaplot comparing cfDNA enrichment at PANC-1 enhancer and promoter regions. Mean enrichment profiles of cfDNA from pancreatic cancer patients and healthy controls are plotted.

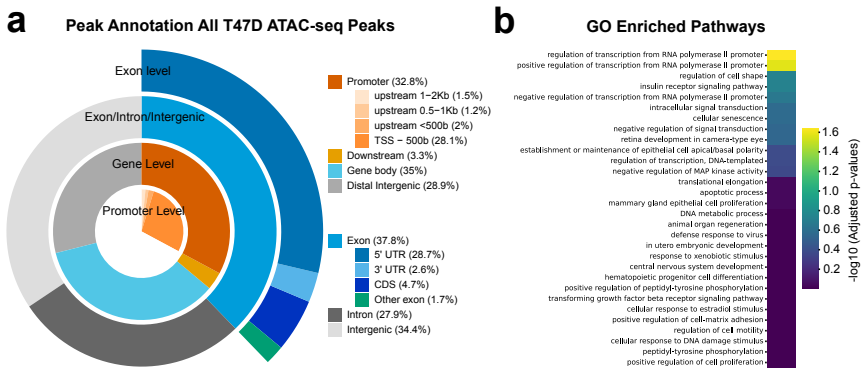

Supplementary Figure 2. Breast cancer cfDNA analysis using luminal breast cancer open chromatin.

a. Peak annotation of all T47D ATAC-seq peaks. Peaks are categorized into various groups, including promoter, exon, intron, and intergenic regions. **b.** Gene ontology (GO) analysis. Differential peaks from breast cancer cfDNAs were assigned to nearest genes and GO biological process pathway analysis was conducted to identify associated biological pathways.

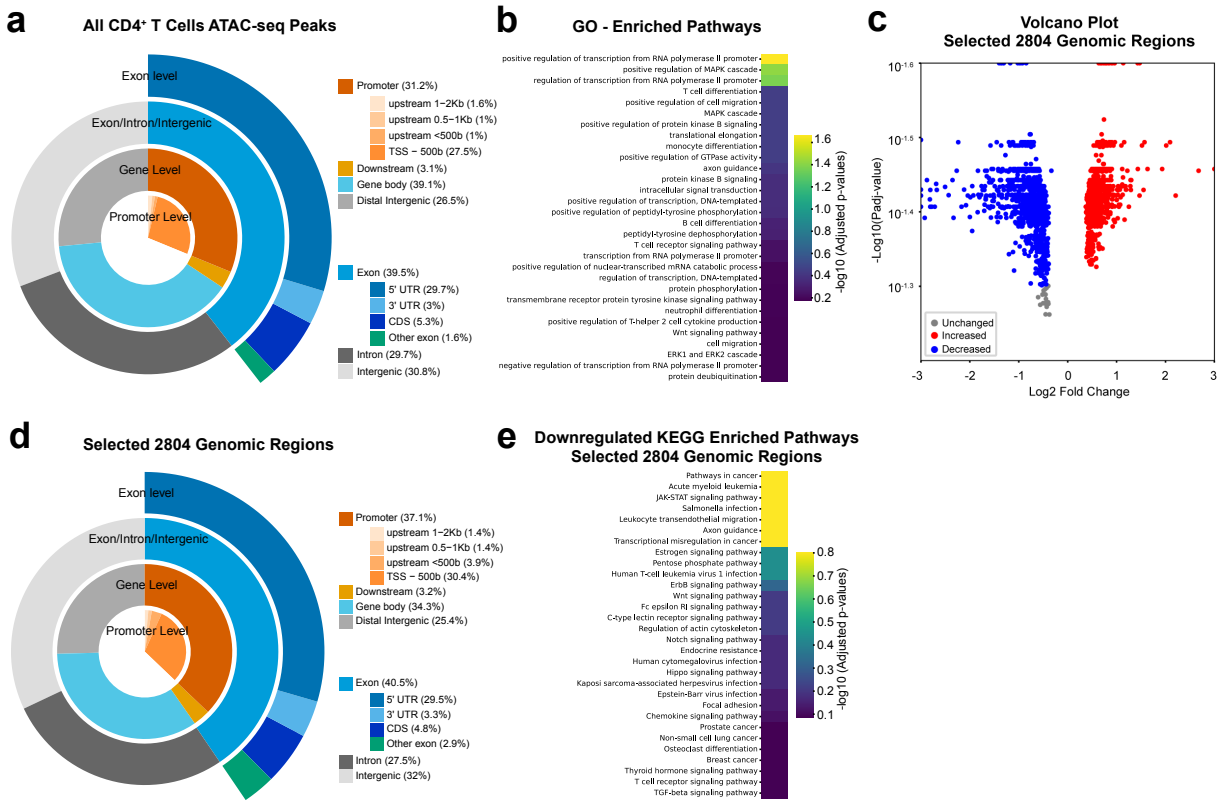

Supplementary Figure 3. cfNuc enrichment analysis using both luminal and immune cell ATAC-seq peaks.

a. Peak annotation of CD4$^+$ T cell ATAC-seq peaks. Doughnut chart showing the distribution of ATAC-seq peaks across different genomic regions such as promoters and gene bodies. **b.** Top significant GO pathways associated with differential loci found at CD4$^+$ T cell ATAC-seq peaks. **c.** Volcano plot showing cfNuc signal differences at the union (2,804) differential peaks. **d.** Peak annotation of 2,804 union genomic regions. **e.** KEGG pathways enrichment analysis of genes associated with decreased cfDNA signals in luminal breast cancer.

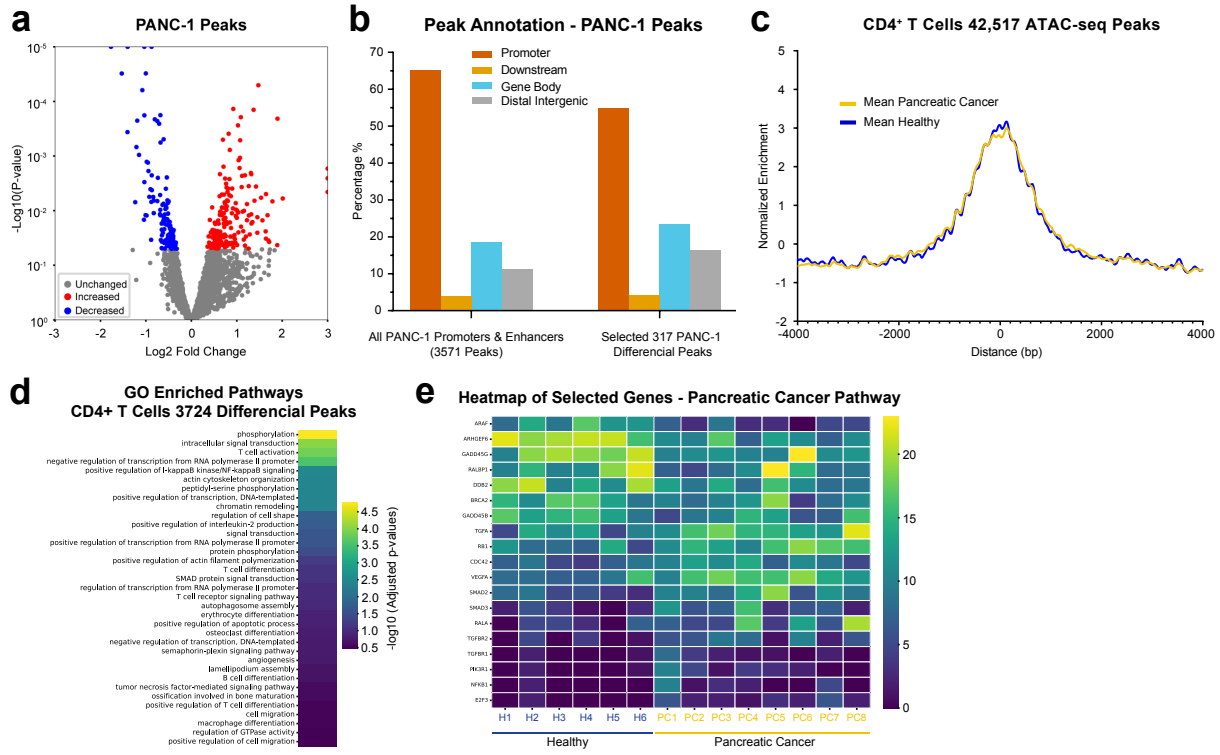

Supplementary Figure 4. Pancreatic cancer cfDNA analysis.

a. Volcano plot for differential peak analysis using cfDNAs isolated from pancreatic cancer. **b.** Peak annotation of all PANC-1 promoters and enhancers (left), and differential peaks found in cfDNAs derived from pancreatic cancer patients (right). **c.** Metaplot showing mean cfDNA enrichment in pancreatic cancer patients at CD4⁺ T cell ATAC-seq peaks. **d.** GO pathway analysis from 3,724 differential peaks found at CD4⁺ T cell ATAC-seq peaks. **e.** Heatmap showing expression levels of genes associated with pancreatic cancer pathway. Normalized read counts collected from each CD4⁺ T cell ATAC-seq peak are depicted as gene expression values.

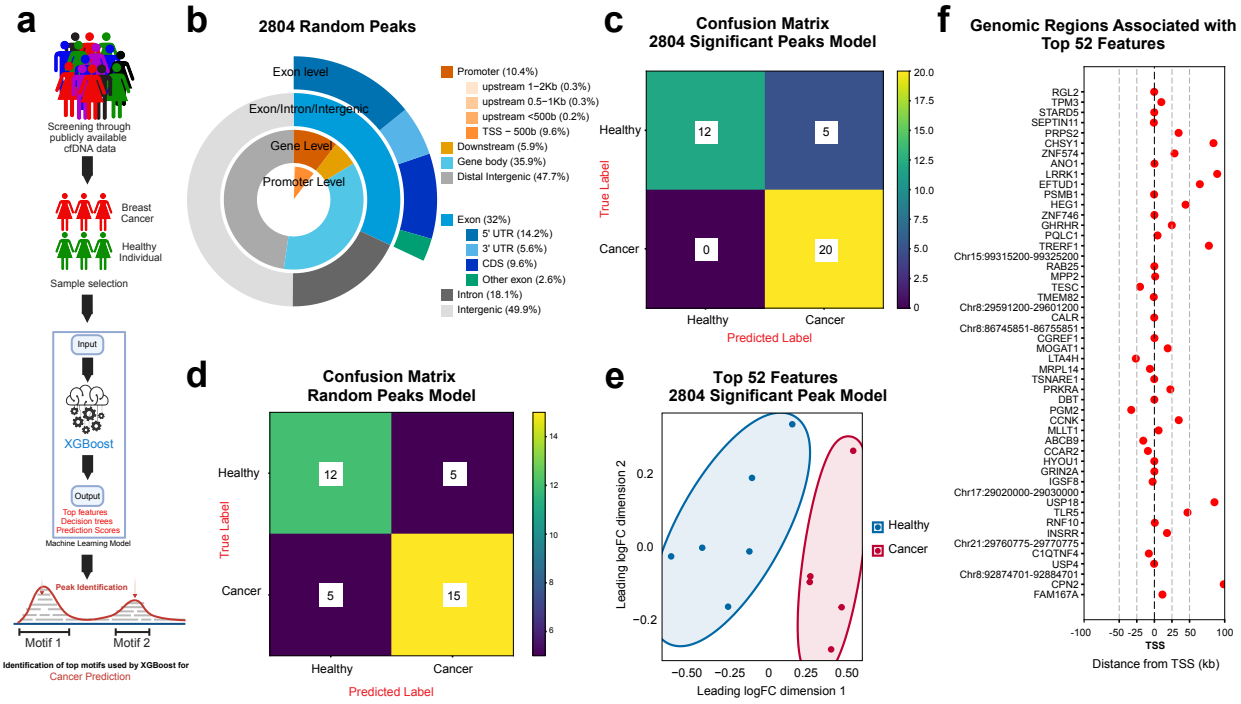

Supplementary Figure 5. Predictive analysis and feature interpretation using XGBoost machine learning.

a. Sample selection and data processing workflow for cfDNA analysis using XGBoost**.** **b.** Peak annotation of 2,804 randomly selected regions. Compared to 2,804 differential peaks found in breast cancer cfDNAs, promoter regions are slightly less frequent. **c.** Confusion matrix showing prediction results from an XGBoost-trained model. The model was established using publicly available cfDNA data, focused exclusively on 2,804 differential loci found in breast cancer cfNuc data. **d.** Confusion matrix from the XGBoost-trained model using randomly selected genomic loci. **e.** PCA plot demonstrating clear separation of cfDNA profiles between healthy and breast cancer samples. Our cfDNA data were used for validation. Read counts were collected in the top 52 features identified by the XGBoost model. **f.** Distribution of the top 52 genomic features relative to TSS.